

Characterization of relief printing

Xing Liu^a, Lin Chen^b, Maria-Valezzka Ortiz-Segovia^c, James Ferwerda^b, and Jan Allebach^a

^aSchool of Electrical and Computer Engineering, Purdue University, 465 Northwestern Avenue, West Lafayette, IN 47907-2035, United States

^bMunsell Color Science Laboratory, Chester F. Carlson Center for Imaging Science, Rochester Institute of Technology, Rochester, NY 14623, United States

^cOcé Print Logic Technologies, 1 rue Jean Lemoixne, 94015 Créteil, France

ABSTRACT

Relief printing technology developed by Océ allows the superposition of several layers of colorant on different types of media which creates a variation of the surface height defined by the input to the printer. Evaluating the reproduction accuracy of distinct surface characteristics is of great importance to the application of the relief printing system. Therefore, it is necessary to develop quality metrics to evaluate the relief process. In this paper, we focus on the third dimension of relief printing, i.e. height information. To achieve this goal, we define metrics and develop models that aim to evaluate relief prints in two aspects: overall fidelity and surface finish. To characterize the overall fidelity, three metrics are calculated: Modulation Transfer Function (MTF), difference and root-mean-squared error (RMSE) between the input height map and scanned height map, and print surface angle accuracy. For the surface finish property, we measure the surface roughness, generate surface normal maps and develop a light reflection model that serves as a simulation of the differences between ideal prints and real prints that may be perceived by human observers. Three sets of test targets are designed and printed by the Océ relief printer prototypes for the calculation of the above metrics: (i) twisted target, (ii) sinusoidal wave target, and (iii) ramp target. The results provide quantitative evaluations of the printing quality in the third dimension, and demonstrate that the height of relief prints is reproduced accurately with respect to the input design. The factors that affect the printing quality include: printing direction, frequency and amplitude of the input signal, shape of relief prints. Besides the above factors, there are two additional aspects that influence the viewing experience of relief prints: lighting condition and viewing angle.

Keywords: relief printing, printing quality, MTF, light reflection model

1. INTRODUCTION

Conventional printers are constrained to reproduce image content in a two-dimensional space as they are not capable of using any height or surface information that may exist in a third dimension. Relief printing technology developed by Océ allows the superposition of several layers of ink on different types of media, which creates a variation of the surface height defined by the input to the printer. Relief printing opens the possibility to create texture patterns to enhance a print's appearance, which has significant applications in the reproduction of artwork and the production of packaging, signage, and decorative materials.

The printing accuracy and surface appearance are of great importance to further development and application of relief printing. Therefore, it is necessary to develop quality metrics to evaluate the relief process. Over the last several decades, much research has been done on 2D image quality assessment¹⁻⁶ and work has been done to evaluate the quality of 3D prints, objects, or computer simulations.⁷⁻⁹ However, no image quality metrics have been defined for 2.5D prints. Some initial thoughts might start with the connections between 2.5D prints and 2D images, as well as 3D objects. On the one hand, considering the fact that 2.5D prints present different appearances depending on the illumination environment and the viewer's position relative to the print and the illumination, each appearance can be interpreted as a 2D scene, which can be evaluated with 2D image quality metrics. Similar approaches have been seen in 3D scene evaluations.¹⁰ On the other hand, shape and surface texture are key aspects in both 2.5D and 3D printing characterization. Hence, parallels can be made between reproduction accuracy of 2.5D prints and that of 3D prints.

Further author information: (Send correspondence to Xing Liu.)
Xing Liu: E-mail: liu192@purdue.edu

In this paper, we attempt to objectively evaluate the relief printing process in the third dimension, i.e. height information. To achieve this goal, we define metrics and develop models that aim to assess relief printing quality in two aspects: overall fidelity and surface finish. For the overall fidelity, three metrics are calculated: modulation transfer function (MTF), difference and root-mean-squared error (RMSE) between the input height map and scanned height map, and print surface angle accuracy. To characterize the surface finish property, we measured the surface roughness, generated surface normal maps, and developed a light reflection model that serves as a simulation of the difference that may be perceived by human observers between ideal prints and real prints. Three sets of test targets were designed and printed by the Océ relief printer prototype for the calculation of the above metrics: (i) twisted target, (ii) sinusoidal wave target, and (iii) ramp target. The twisted target and ramp target were designed to evaluate both the overall fidelity and the surface finish. We choose suitable metrics or models for the two targets, respectively, according to their surface pattern features. The sinusoidal wave target was used only for the MTF calculation as a probe to the overall fidelity.

The rest of this paper is organized as follows. Section 2 gives a brief introduction to relief printing. Following that, three sets of test targets are presented in Sec. 3. The quality metrics are described in Sec. 4 and their results presented in Sec. 5. In Sec. 6, this paper ends with some conclusions and suggestions for future work.

2. RELIEF PRINTING AND SCANNING METHODS

Similar to the 2D printing technology, the surface color of relief prints is defined by a color image sent to the printer. Beyond that, to define the surface height, a height map of the same size as the color image is generated as a second input to the printer. The height map is a grey level map with its pixel values determining the relative height at each pixel in the final print.

We work with two Océ prototype printers that produce relief prints. Two inkjet technologies are used, which we refer to as wet-on-wet and wet-on-dry printing. Each of them produces a distinct type of surface relief, and is used for different applications. One difference between the two printers is that the wet-on-dry printer uses UV curable ink and can print higher altitudes than the wet-on-wet printer. Another difference between the two printers is that the final print height is predictable with the wet-on-dry printer, but not with the wet-on-wet printer.

The estimated final print height printed by the wet-on-dry printer can be calculated by the following equation

$$A = H \times TU, \quad (1)$$

where A is the desired print height, H is the number of the specified unit values, and TU is the thickness unit with a value $8.6 \mu\text{m}$ for the target print engine. The value of H is determined as follows: The minimum value of H is fixed to be 0 and the maximum value of H is denoted as H_{MAX} , which is to be determined by the user. By mapping the digital pixel values in the input height map to $[0, H_{MAX}]$, we get the value of H for every pixel. Following the calculation using Eq. (1), the input height map can be translated to a desired height map with element units of μm .

Two scanning methods are used to obtain the height map of the prints. The first scanning method uses the LMI Gocator* of which the output is a direct height map. The resolution is $0.017 - 0.049$ mm along the scanning direction and $0.190 - 0.340$ mm along the direction of the sample movement. The second scanning method measures surface texture characteristics using a 2D flatbed scanner Canon 5600F.^{11,12} It returns a height map with low resolution and is not characterized to provide measurements in physical units. Hence the measurement can only be used for comparison between targets. We will refer the unit as ‘measurement unit’ in the following.

In this paper, we are interested in print quality in the height dimension. The surface height variation of the final print is scanned to generate a height map, from which we develop metrics either with or without reference to the input height map.

3. TEST TARGETS

There are three sets of targets designed and printed by one or both relief printing technologies. In the following, we introduce each test target by showing its height map, as well as the scanning method used to characterize the resulting print.

*LMI Technologies Inc., 1673 Cliveden Ave. Delta, BC Canada.



Figure 1. Height map of twisted target, which is to be printed by the wet-on-dry printer.

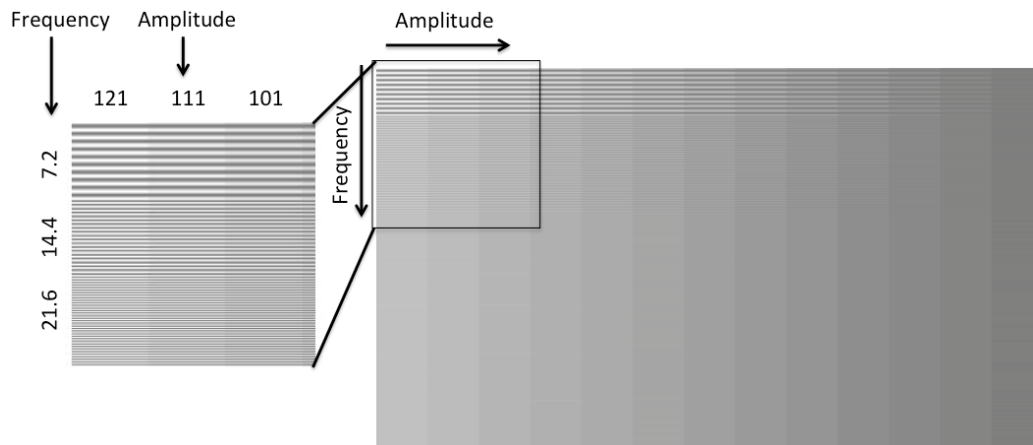


Figure 2. Sinusoidal wave target set I designed for the measurement of MTF, which is to be printed by the wet-on-dry printer.

3.1 Twisted target

The twisted target has the height map shown in Fig. 1. It is printed by the wet-on-dry printer and scanned by the LMI Gocator. It is designed to measure the overall fidelity of the relief printing.

3.2 Sinusoidal wave target

The sinusoidal method, which uses a set of sinusoidal wave targets at different frequencies and amplitudes, is widely used to measure the MTF of printing devices.^{13,14} We designed two sets of sinusoidal targets for this purpose. Set I was designed to characterize the wet-on-dry printer and to be scanned by the LMI Gocator. It contains an 8×13 array of square sinusoidal patches. The frequency and amplitude of the patches vary across the target as shown in Fig. 2. One column consists of frequencies from 7.2 cycles/inch to 57.6 cycles/inch with a step of 7.2 cycles/inch and one row consists of amplitudes from 1 unit of digital value to 121 unit of digital value with a step of 10.





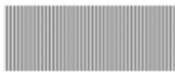
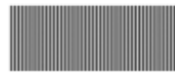



A second set of sinusoidal targets was designed to characterize the wet-on-wet printer, and consisted of 9 patches with frequencies of {30, 50, 80} cycles/inch and amplitudes of {42, 84, 126} digital values. A subset of these height maps is shown in Fig. 3.

3.3 Ramp target

The ramp target was designed to measure the angular accuracy and light reflection properties of the wet-on-dry printer. One test page of the ramp target contains one column of cylinder-shaped patches and 8 columns of ramp-shaped patches. Its height map is shown in Fig. 4. The height map of the real prints is obtained by using the flatbed scanner.

4. QUALITY METRICS AND RESULTS

Just as with 2D printing, there are always differences between the input digital files and the printed samples. Height information is an important component of the relief prints. So an in-depth analysis of the height accuracy problem for

Parameters	Amplitude *: [0, 84]	Amplitude : [0, 168]	Amplitude : [0, 252]
Frequency: 30 cpi	1 	2 	3 
Frequency: 50 cpi	4 	5 	6 
Frequency: 80 cpi	7 	8 	9 

* Amplitude is in digital values.

Figure 3. Sinusoidal wave target Set II designed for measurement of MTF, which is to be printed by the wet-on-wet printer.

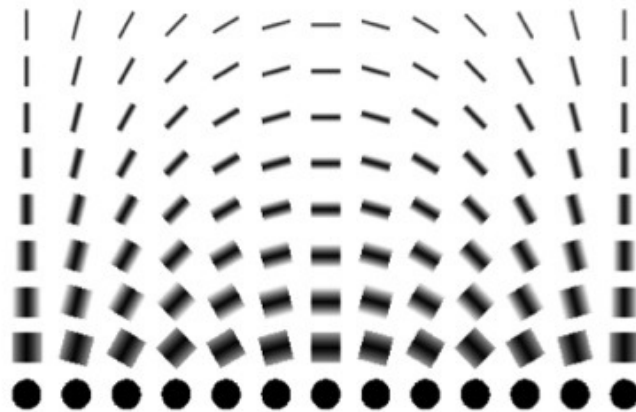


Figure 4. Ramp target designed to measure the angle accuracy of structures in 2.5D prints made with the wet-on-dry printer.

relief printing is necessary. Quality metrics are used to give an objective evaluation of the printing quality, and can be used for the computation of printer compensation and adjustments.

We considered two approaches to assess the relief printing quality. The first approach deals with the accurate reproduction of the input digital image file, i.e. overall fidelity. To evaluate this aspect, we adopted three metrics: MTF, difference and RMSE, and print surface angle accuracy. The second approach is related to the surface finish of the relief prints, for which we measured the surface roughness, generated surface normal maps and developed a light reflection model that serves as a simulation of the difference between ideal prints and real prints that may be perceived by human observers. In the following sections, these approaches and metrics will be introduced in detail.

4.1 Overall fidelity

4.1.1 Modulation transfer function - MTF

The MTF of a printing system is a function of frequency or amplitude characterizing how much the system attenuates an input modulation signal.^{13,14} A few methods have been developed to measure the MTF of 2D digital image reproduction devices, including the sinusoidal method, slanted-edge method, and grill method. In this paper, we applied the sinusoidal method to evaluate the height modulation of the sinusoidal wave targets. We measure the MTF as a function of frequency and amplitude to evaluate the ability of a relief printer to reproduce details in height.

The MTF is defined as the ratio of the output modulation $M(Output)$ to the input modulation $M(Input)$:

$$MTF = \frac{M(Output)}{M(Input)}. \quad (2)$$

In this paper, the modulation is defined in the frequency domain

$$Modulation = \frac{2 \times F(k_0)}{F(0)}, \quad (3)$$

where $F(k_0)$ denotes the fundamental frequency component and $F(0)$ the DC component.

4.1.2 Difference and RMSE

The mean absolute difference and RMSE are used commonly in 2D image comparison and 3D printing quality evaluation.^{2,7} Here, we calculate the difference and RMSE between the desired height map and the scanned height map. By these two metrics, we aim to have an overall assessment of how strongly the printed heights deviate from the desired heights.

This metric is only applicable for the wet-on-dry printer, since the desired height can be calculated by Eq. (1) for the wet-on-dry printer. However, there is no such height mapping equation for the wet-on-wet printer.

The mean absolute difference between two height maps of size $M \times N$ is defined as:

$$MAD = \frac{1}{MN} \sum_{i=1}^M \sum_{j=1}^N |(I_{ij}^D - I_{ij}^S)|, \quad (4)$$

where I_{ij}^D denotes the desired height map and I_{ij}^S the scanned height map. On the other hand, RMSE is defined as:

$$RMSE = \sqrt{\frac{1}{MN} \sum_{i=1}^M \sum_{j=1}^N (I_{ij}^D - I_{ij}^S)^2}. \quad (5)$$

4.1.3 Print surface angle

The ramp target was designed to measure the angular accuracy of the relief prints. We have calculated four metrics: *leftangle*, *rightangle*, *peakheight* and *bottomwidth*. With the scanned height map, surface slices are taken as shown in Fig. 5(a) along the indicated direction. An average slice is calculated as the mean of all the slices. We fit the average slice with a straight line, and then calculate the four metrics that are illustrated in Fig. 5(b). The reason why we separate the left angle from the right angle is that there might exist asymmetries in the prints, which can be explored by comparing the two angles.

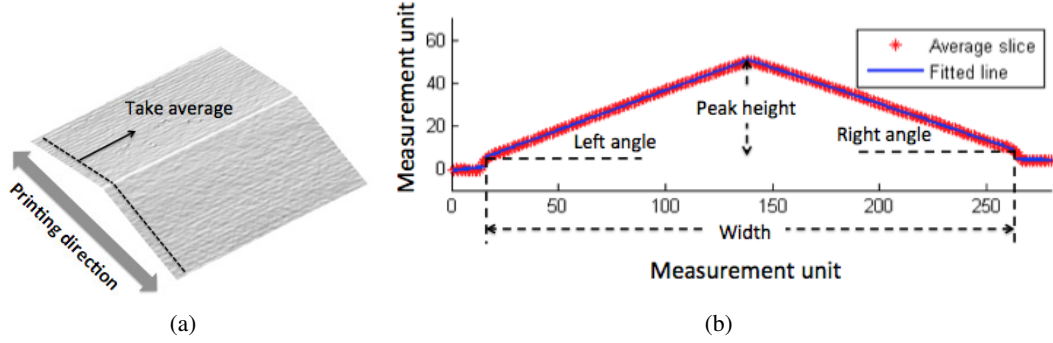


Figure 5. (a) Surface slices on the ramp target are taken as shown in the dashed line along the direction indicated by the arrow. (b) Definitions of the four metrics: left angle, right angle, peak height, and width.

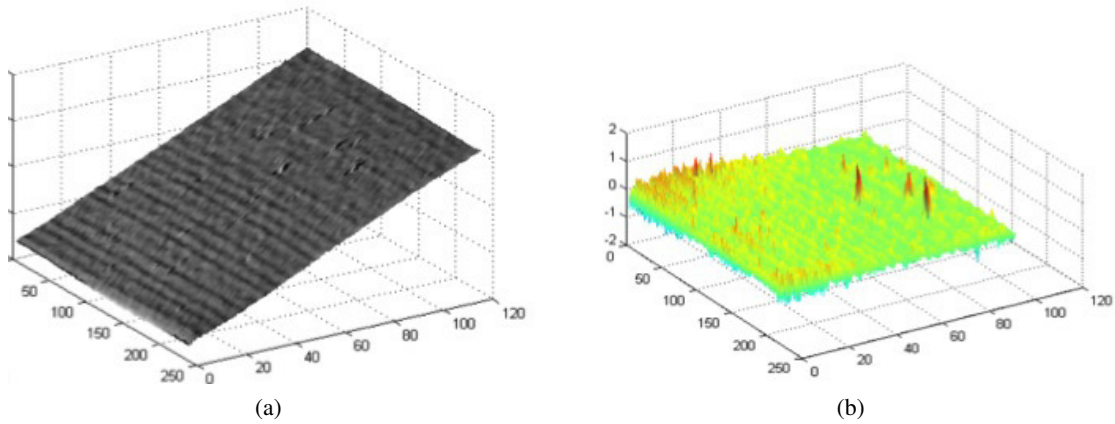


Figure 6. (a) Surface of interest for the ramp target. The height of the surface is in measurement units. (b) Surface roughness profile in measurement units.

4.2 Surface finish

4.2.1 Surface roughness

Surface texture plays an important role in the appearance of prints.¹⁵ The metric developed in this section serves as a measure of the texture of the surface.

Our approach extends the ISO standard¹⁶ for line raggedness to 2D to take the entire relief print surface into account. For a surface of interest, such as that shown in Fig. 6(a), we generate a surface roughness profile by applying a 2D high pass filter to it, as shown in Fig. 6(b). We then calculate the difference between the surface roughness profile and its mean to obtain a 2D residual plane of size $M \times N$, which is denoted by e_{ij} . Two metrics are calculated: the first one is the root mean square value of the 2D residual; and the second one is the maximum among the residuals.

$$R_{RMS} = \sqrt{\frac{1}{MN} \sum_{i=1}^M \sum_{j=1}^N e_{ij}^2}, \quad (6)$$

$$R_{MAX} = MAX(e_{ij}). \quad (7)$$

4.2.2 Surface normal

The surface normal vectors affect the light reflection, and hence the appearance, of the surface. We are interested in depicting the surface texture characteristics by computing the normal vectors from the height maps.

Our approach is to generate a surface normal map by rescaling each of the x , y , and z components of the surface normal vectors to $[0, 255]$ and using the rescaled x , y , and z components as the R, G, and B values in the RGB color space of the surface normal map. By this conversion, the x , y , and z components of the surface normal vectors are transferred to R, G, and B values and can be visually displayed as the surface normal map. This surface normal map provides a visual description of the print surface texture and a comparison to the desired surface texture calculated from the input height map.

4.2.3 Light reflection simulation

Relief prints are different from 2D prints in that they have surface height variation, which leads to varying visual experiences under different viewing conditions including the incident illumination, and different print properties, such as the surface Bi-directional Reflectance Distribution Function (BRDF), and the surface normal.^{17–20} We simulate the surface appearance by calculating the light reflection from the height map using the Phong reflection model.²¹ Furthermore, with the input height map and the scanned height map, we are able to simulate both the input and printed appearance and compare the difference between them. To extract metrics that describe the difference, we calculate the difference between the input and output light reflection. A threshold is applied to the absolute value of the difference; so we can select out the high difference values that would capture our attention. We call the values that are above the threshold ‘peaks’, and the ones that are below the threshold ‘background’.

Four metrics are developed based on the absolute light reflection difference, which we denote as D_{ij} . The first one is the root mean square value of the difference D_{ij} between the input and the scanned height maps. The second one is the contrast, which is defined as the ratio of the sum of the peak values to the sum of the background values. The third metric is called density for which we take the sum of the peak values divided by the area of the peaks. The last metric is the density contrast which is the ratio of the density of the peaks to the density of the background.

Table 1. Four metrics based on the light reflection calculation.

Root Mean Square Error	$\sqrt{\frac{1}{MN} \sum_{i=1}^M \sum_{j=1}^N D_{ij}^2}$
Contrast	$\frac{\sum \text{Peak values}}{\sum \text{Background values}}$
Density	$\frac{\sum \text{Peak values}}{\sum \text{Peak area}}$
Density Contrast	$\frac{\text{Density of the Peaks}}{\text{Density of the Background}}$

5. RESULTS

5.1 Overall fidelity

5.1.1 Modulation transfer function - MTF

We calculated the MTF for the sinusoidal wave target set I printed by the wet-on-dry printer; and the result is shown in Figs. 7(a) and 7(b). It can be seen in Fig. 7(a) that the MTF decreases as the spatial frequency of the target increases. The result only shows the MTF for frequencies under 45 cycles/inch, as the measurement contains too much noise when the frequency exceeds 45 cycles/inch and no principle component could be selected from the Fourier Transform. The frequencies where the MTF drops below 0.5 can be considered as cutoff frequencies for the printer to reproduce fine details. We also observe dependence of the MTF on the input amplitude in Fig. 7(b). At frequencies lower than 30 cycles/inch, the MTF decreases with increasing amplitude. However, at around 30 cycles/inch, the MTF shows no dependence on the amplitude and remains near a low value of 0.25. Other than the noise introduced by the printing process, the poor performance of the MTF at high frequencies may also be due to the low scanning resolution and quality. One data point appears to be an outlier, possibly due to errors in the data acquisition: in Figs. 7(a) and 7(b) on the curve for amplitude 81 at 7.2 cycles/inch. A better scanning method and scanner calibration might resolve this issue.

The MTF for the sinusoidal wave target set II printed by the wet-on-wet printer is shown in Figs. 8(a) and 8(b). From Fig. 8(a) we can see that the MTF decreases with increasing frequency and is as low as 0.1–0.2 at 80 cycles/inch.

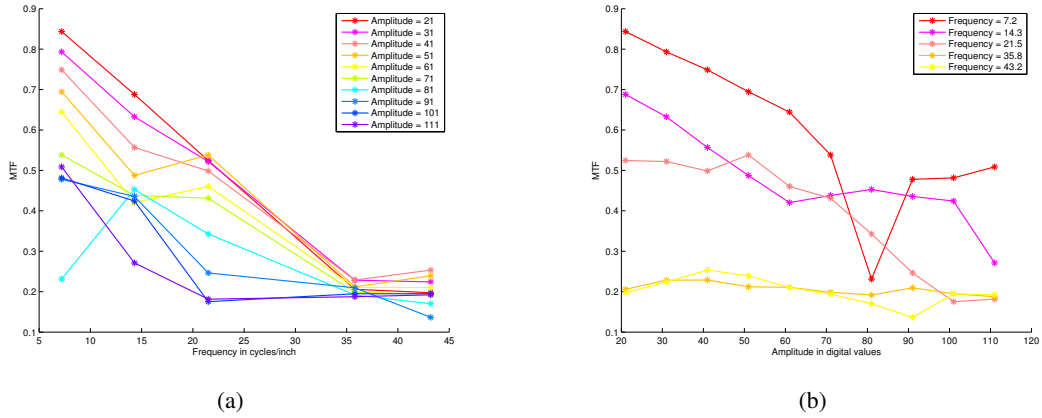


Figure 7. MTF for part of sinusoidal wave target set I printed by the wet-on-dry relief printer. (a) MTF as a function of frequency for 10 fixed amplitudes. (b) MTF as a function of amplitude for 5 fixed frequencies.

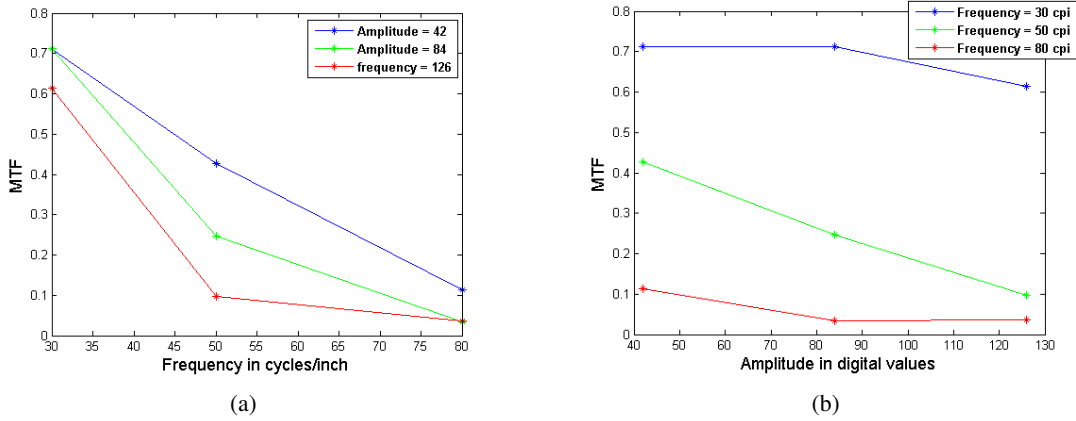


Figure 8. MTF for sinusoidal wave target set II printed by the wet-on-wet relief printer. (a) MTF as a function of frequency for 3 fixed amplitudes. (b) MTF as a function of amplitude for 3 fixed frequencies.

Figure 8(b) shows how the input amplitude affects the MTF. It reveals that the amplitude has a larger influence on MTF when the frequency of the signal is around 50 cycles/inch. The performance is consistently good at the low frequency (30 cycles/inch) and consistently poor at the high frequency (80 cycles/inch).

5.1.2 Difference and RMSE

Difference and RMSE are calculated for the twisted target printed using the wet-on-dry printer. Figure 9 shows a difference map obtained by subtracting the scanned height map from the desired height map. For most of the area in the difference map, the difference is negative meaning that according to the scanned data, the final print is mostly higher than the desired print. This is due to the fact that the height mapping equation Eq. (1) is just an approximation to the final print height and needs to be calibrated. If more data were available, the height difference from our calculation could be used to adjust the height mapping equation. We also observe red regions along the edges and at the corners of the twisted target prints in Fig. 9, which indicates that the prints are attenuated more in those areas than in the center areas.

Table 2 gives the results of the two metrics for the twisted target printed with the wet-on-dry printer. The height range of the scanned height is 0.117 – 2.675 mm; so we can conclude that the values of the mean absolute difference and RMSE are small. Although there are fluctuations over the whole print, the height is mostly reproduced with a low percentage error.

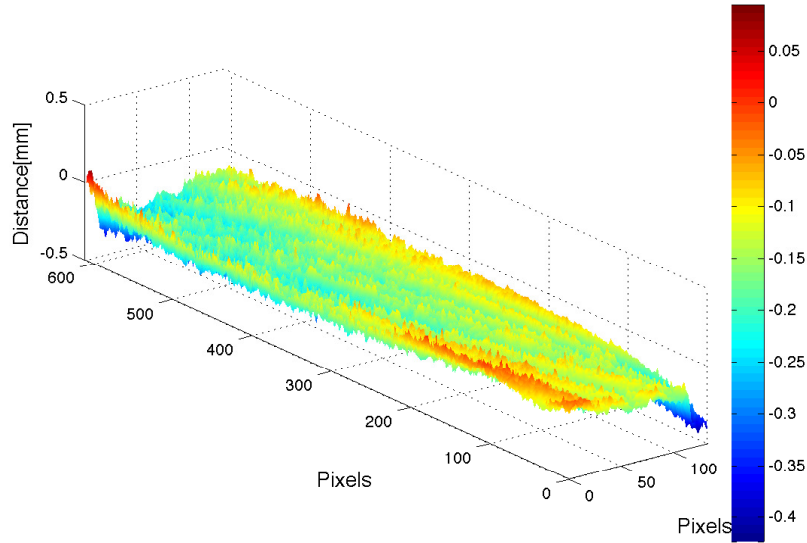


Figure 9. Difference map for the twisted target printed using the we-on-dry printer. It is calculated by subtracting the scanned height map from the desired height map.

Table 2. Mean absolute difference and RMSE for the twisted target.

Metric	Absolute Value	Relative Error [†]
Mean absolute difference	0.174 mm	6.49%
RMSE	0.182 mm	6.81%

[†] (Absolute value divided by range) \times 100

5.1.3 Print surface angle

With the limited scanning data, we compared the angular accuracy for the ramp targets shown in Fig. 10 that were printed using the wet-on-dry printer. The results are shown in Fig. 11. Note that the ramps are designed as follows: From Ramp 1 to Ramp 7, the target angles increase linearly, the bottom widths decrease linearly, and the peak heights remain the same.

In Fig. 11(a) we see a nearly linear increase in angle from Ramp 1 to Ramp 7. The left angles are always slightly larger than the right angles, which indicates a constant asymmetry in the geometry of the prints. The variance in peak heights across the 7 ramps shown in Fig. 11(b) is small. In Fig. 11(c), the width drops nearly linearly from Ramp 1 to Ramp 7. From the results, we conclude that there exists a position dependence on the printing direction of the geometry of the relief prints.

5.2 Surface finish of relief prints

5.2.1 Surface roughness

Surface roughness is calculated for the ramp targets shown in Fig. 10. It is calculated separately for the left and right parts. Two histograms are generated for the values of R_{RMS} and R_{MAX} , as shown in Figs. 12(a) and 12(b). Both metrics show an increasing trend from Ramp 1 to Ramp 7, indicating that the surface becomes rougher as the slope becomes steeper. But it is worth noting that in Fig. 12(b), which shows the maximum of the residuals, Ramp 2 has a very high value. This is due to a significant local print artifact in Ramp 2. But this local defect is not picked out in the RMS value of the residuals. To determine which metric to use, a psychophysical experiment is needed to relate the metric values to human perception.

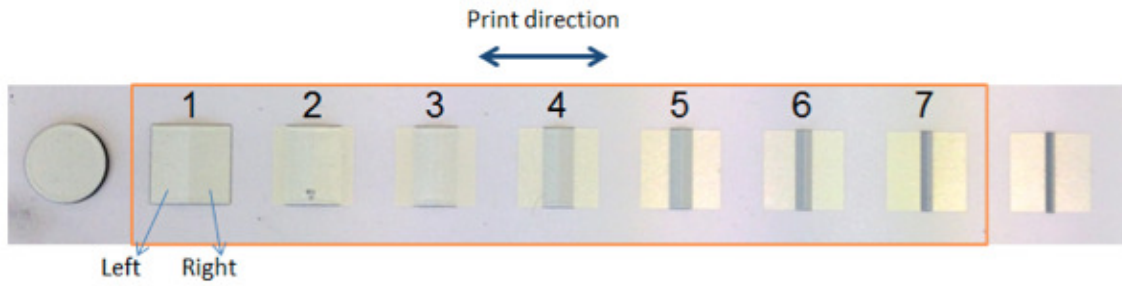


Figure 10. Ramp targets used for calculation of angular accuracy. This is an image of the targets that have been printed using the wet-on-dry printer. The left and right side are defined as noted.

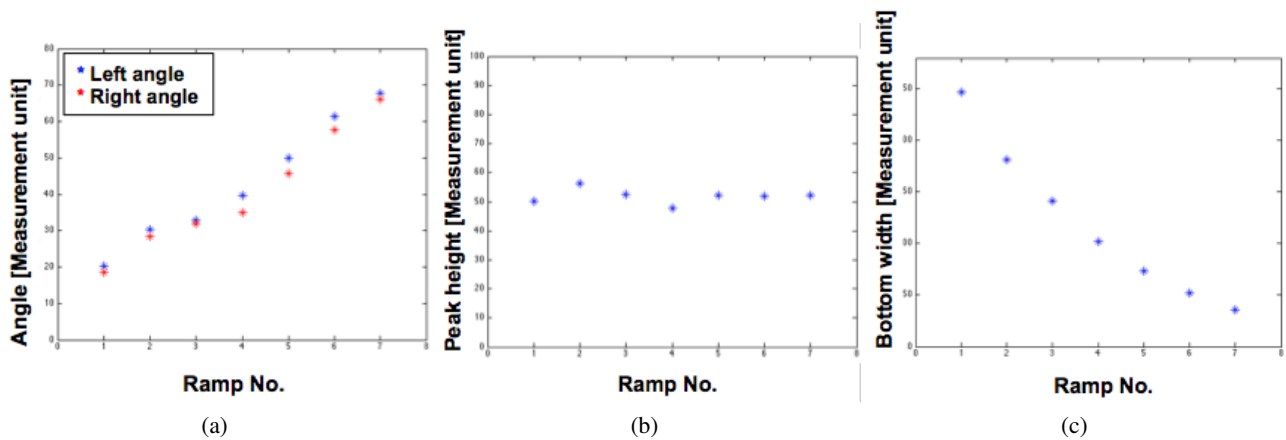


Figure 11. Measurement for the ramp target shown in Fig. 10 printed with the wet-on-dry printer. (a) angles, (b) peak height, and (c) width.

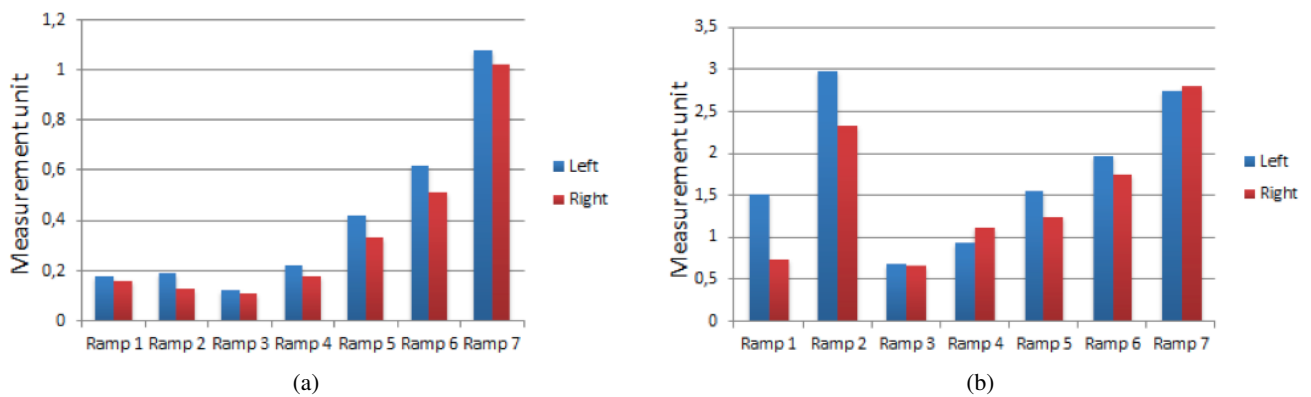


Figure 12. Residuals for the ramp target shown in Fig. 10 printed with the wet-on-dry printer: (a) RMS value of the residuals, (b) Maximum value of the residuals.

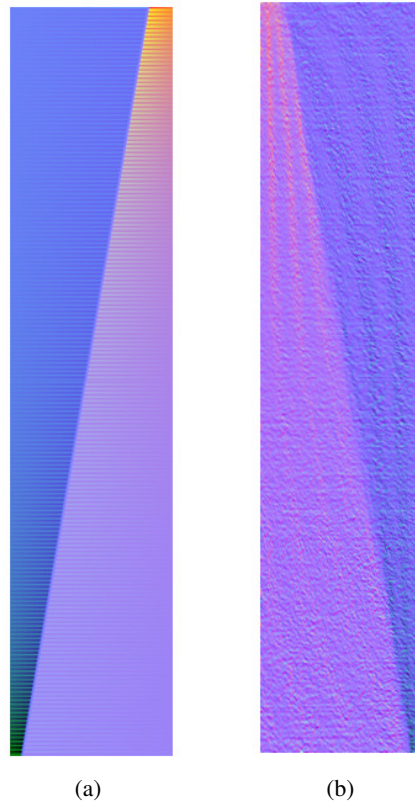


Figure 13. Surface normal maps for the twisted target: (a) From the input height map. (b) From the scanned height map of the twisted target printed by the wet-on-dry printer.

5.2.2 Surface normal

The surface normal maps are generated for the twisted target for both the input height map and the scanned height map obtained from the twisted target printed with the wet-on-dry printer. The result is shown in Fig. 13(a), which provides a visualization of the surface normal vectors. The curved banding pattern in the surface normal map from the scanned data depicts the surface roughness of the real print. This variation aligns very well with our observation of the real print. By comparing with the surface normal map from the input data, we can describe what the differences are and the shape and location of artifacts.

5.2.3 Light reflection simulation

We applied light reflection simulation to the ramp targets printed by the wet-on-dry printer, aiming to obtain a heuristic visualization of the surface characteristics for both the ideal and real prints. Some comparisons are provided in Fig. 14 between the surface appearance of the photo of the real print, the light reflection simulation based on the scanned height map, and the one based on the input height map. With limited control of the experimental environment, we tried our best to match the light direction and color between each photo and the corresponding simulation. We can see that the light reflection simulations work well to match the photos of the real print. As expected, the same print exhibits different surface appearances under different lighting conditions and viewing angles. The defects that are obvious under a certain lighting condition might not be visible if the illumination direction changes. We expect that the light reflection simulation can provide a fast mean for visualization of the real prints from the scanned measurements.

The four metrics based on the light reflection calculation for Ramp 1 to Ramp 7 are presented in the histograms in Fig. 15. Of the four metrics, the density metric yields a very similar result to the RMS value of the residuals in Fig. 12(a) that describes the surface roughness. As the slope of the ramps becomes steeper, the values of the metrics increases. Again, Ramp 2 stands out in the values of the RMS, density, and density contrast due to the local print defect. Among the four

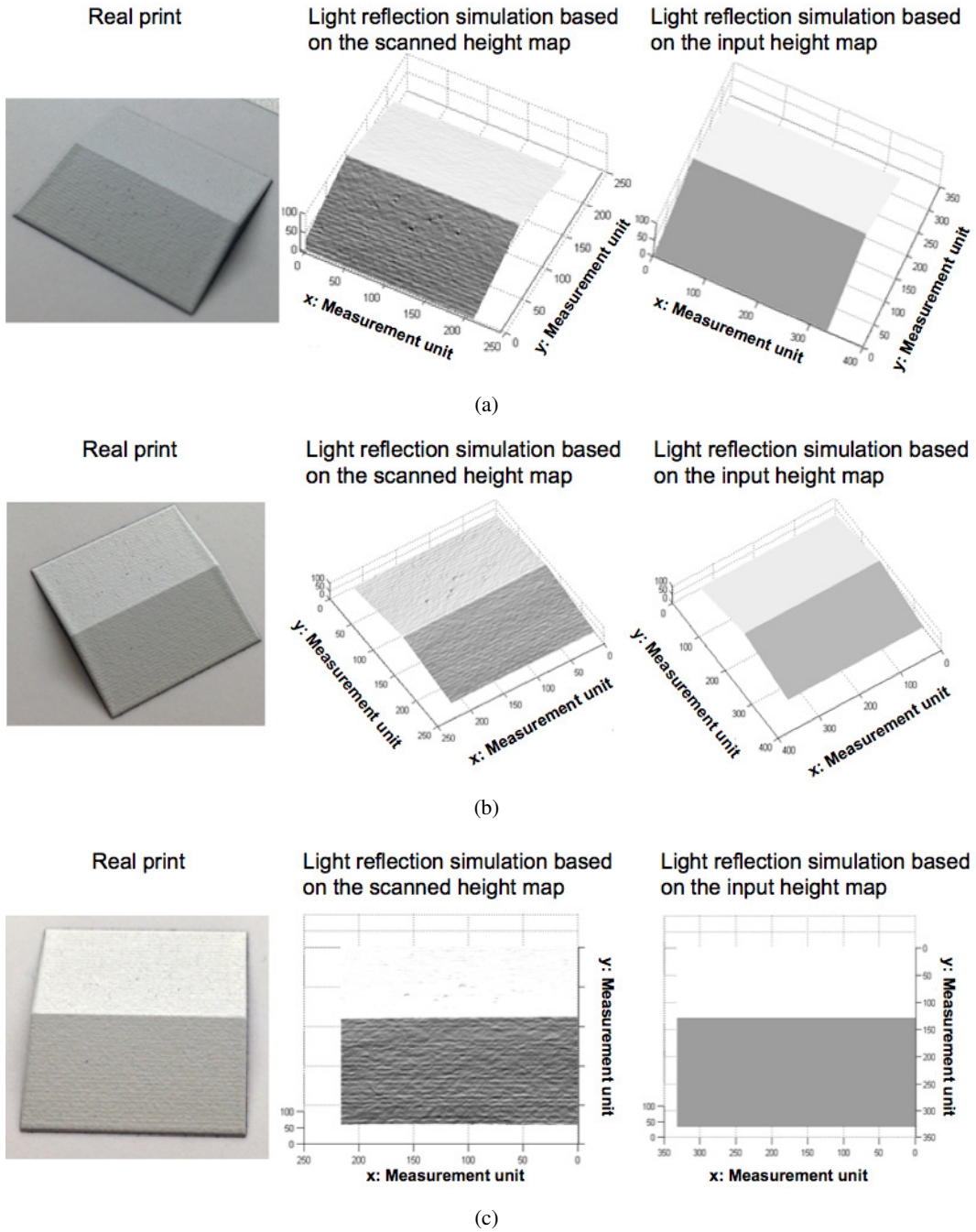


Figure 14. Surface light reflection comparison. (a), (b), and (c) are with different lighting conditions and viewing angles.

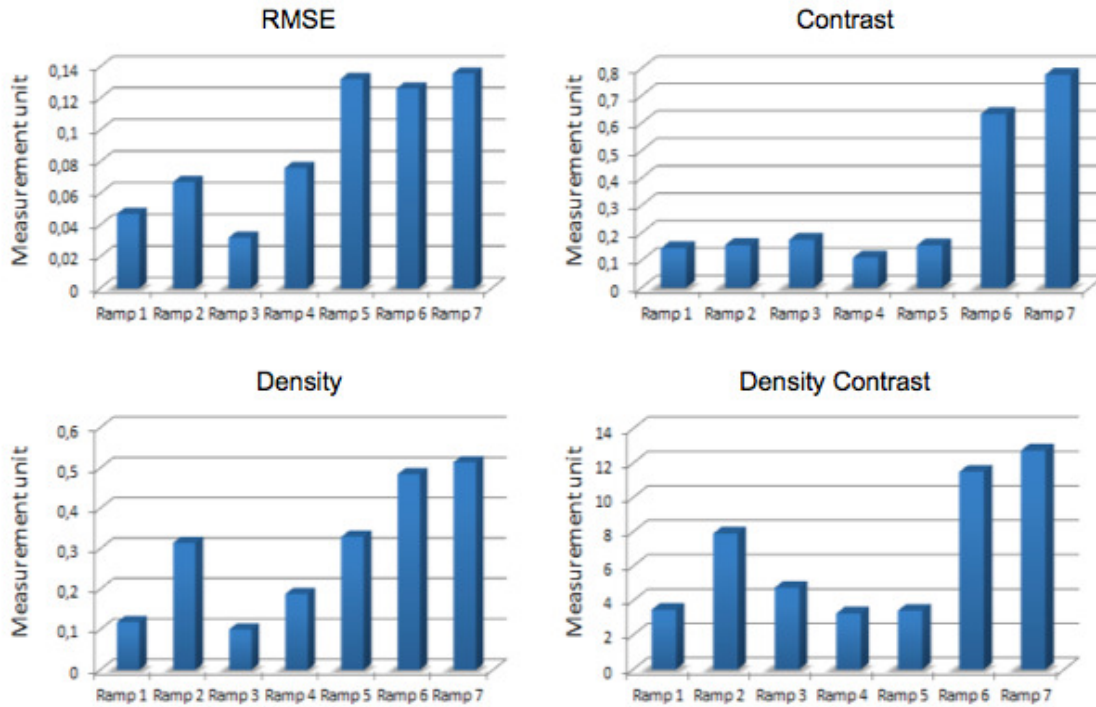


Figure 15. Histograms of the four metrics: root mean square error, contrast, density, density contrast.

metrics, the density metric aligned best with our visual observations. However, as mentioned in the previous section, a psychophysical experiment is desired to measure and validate the metrics we have developed.

6. CONCLUSION AND FUTURE WORKS

In this paper, we have described our work to characterize two relief printers: the wet-on-wet printer and the wet-on-dry printer. In general, the calculated metrics showed that with some exceptions, the relief printers tested reproduced the input designs with good accuracy. However, with the wet-on-dry printer, we observed a dependence on the printing direction. For the ramp target with a symmetric shape along printing direction, the left side is always steeper than the right side. As expected, the MTF analysis shows that there is a strong relationship between the frequency of fine details and the accuracy of the reproduction. The accuracy decreases as the frequency increases. The surface finish analysis leads to the conclusion that the surface roughness depends on the geometry of the relief prints. As the structure of the relief prints becomes steeper, the printed surface becomes rougher. The light reflection model provides a heuristic visualization of the surface characteristics for the ideal prints and the real prints under the same light environment setting. From the simulation we see that the visual experience depends on the direction of the incident illumination and the viewing angle. That is to say, the surface exhibits a different extent of roughness when we change the direction of the incoming light or rotate the relief prints. The above mentioned work provides an initial approach to characterizing relief printers to provide high quality reproduction of surfaces with complex color and 3D texture properties.

A better scanning method is desired to obtain more reliable and robust results. To assess the height reproduction and surface roughness, the scanning method needs to be more accurate and easily calibrated. In order to validate our measurements and equations, psychophysical experiments need to be carried out to find the relationship between numeric values and actual visual perception.

REFERENCES

1. J. Grice and J. P. Allebach, "The print quality toolkit: An integrated print quality assessment tool," *Journal of Imaging Science and Technology* **43**(2), pp. 187–199, 1999.
2. M. Pedersen and J. Y. Hardeberg, "Full-reference image quality metrics: Classification and evaluation," *Foundations and Trends in Computer Graphics and Vision* **7**(1), pp. 1–80, 2012.
3. D. M. Chandler, "Seven challenges in image quality assessment: past, present, and future research," *ISRN Signal Processing* **2013**, 2013.
4. A. K. Moorthy and A. C. Bovik, "Visual quality assessment algorithms: what does the future hold?," *Multimedia Tools and Applications* **51**(2), pp. 675–696, 2011.
5. Z. Wang, A. C. Bovik, H. R. Sheikh, S. Member, and E. P. Simoncelli, "Image quality assessment: From error measurement to structural similarity," *IEEE Trans. Image Processing* **13**, pp. 600–612, 2004.
6. Z. Wang and A. Bovik, "A universal image quality index," *Signal Processing Letters, IEEE* **9**, pp. 81–84, March 2002.
7. D. Dimitrov, W. van Wijck, K. Schreve, and N. de Beer, "Investigating the achievable accuracy of three dimensional printing," *Rapid Prototyping Journal* **12**, pp. 42 – 52, 2006.
8. Y. Pan, I. Cheng, and A. Basu, "Quality metric for approximating subjective evaluation of 3-d objects," *Multimedia, IEEE Transactions on* **7**(2), pp. 269–279, 2005.
9. C. Polzin, S. Spath, and H. Seitz, "Characterization and evaluation of a PMMA-based 3D printing process," *Rapid Prototyping Journal* **19**, pp. 37 – 43, 2013.
10. L. Jin, A. Boev, A. Gotchev, and K. Egiazarian, "3D-DCT based perceptual quality assessment of stereo video," in *Image Processing (ICIP), 2011 18th IEEE International Conference on*, pp. 2521–2524, 2011.
11. R. Pintus, T. Malzbender, O. Wang, R. Bergman, H. Nachlieli, and G. Ruckenstein, "Photo repair and 3D structure from flatbed scanners.," *International Conference on Computer Vision Theory and Applications* , pp. 40–50, 2009.
12. T. Baar and M. V. Ortiz Segovia, "Colour and texture appearance modeling of 2.5D prints.," *AIC Colour 2013, Proceedings of the 12th Congress* , pp. 8–12, 2013.
13. W. Jang and J. P. Allebach, "Characterization of printer MTF," *Journal of Imaging Science and Technology* **50**, pp. 1062–3701, 2006.
14. N. Bonnier and A. J. Lindner, "Measurement and compensation of printer modulation transfer function," *Journal of Electronic Imaging* **19**(1), pp. 011010–011010–22, 2010.
15. M. Yonehara, T. Matsui, K. Kihara, H. Isono, A. Kijima, and T. Sugibayashi, "Evaluation method of surface texture by surface roughness based on geometrical product specifications (GPS)," *Materials Transactions* **45**(4), pp. 1019 – 1026, 2004.
16. I. 13660, "Information technology – office equipment – measurement of image quality attributes for hardcopy output – binary monochrome text and graphic images," ISO 13660:2008(E), International Organization for Standardization and International Electrotechnical Commission, Geneva, Switzerland, 2001.
17. T. Malzbender, R. Samadani, S. Scher, A. Crume, D. Dunn, and J. Davis, "Printing reflectance functions," *ACM Trans. Graph.* **31**, May 2012.
18. F. Pellacini, J. A. Ferwerda, and D. P. Greenberg, "Toward a psychophysically-based light reflection model for image synthesis," in *Proceedings of the 27th Annual Conference on Computer Graphics and Interactive Techniques, SIGGRAPH '00*, pp. 55–64, ACM Press/Addison-Wesley Publishing Co., (New York, NY, USA), 2000.
19. R. Takano, K. Baba, S. Inoue, K. Miyata, and N. Tsumura, "Reproduction of gloss unevenness on printed paper by reflection model with consideration of mesoscopic facet," *Color and Imaging Conference* **2012**(1), pp. 206–210, 2012-01-01T00:00:00.
20. F. B. Leloup, M. R. Pointer, P. Dutré, and P. Hanselaer, "Overall gloss evaluation in the presence of multiple cues to surface glossiness," *J. Opt. Soc. Am. A* **29**, pp. 1105–1114, June 2012.
21. B. T. Phong, "Illumination for computer generated pictures," *Commun. ACM* **18**, pp. 311–317, June 1975.